32

32

SATELLITE & MESOMETEOROLOGY RESEARCH PROJECT

Department of the Geophysical Sciences
The University of Chicago

NSG-333

A SIMPLIFIED GRID TECHNIQUE FOR DETERMINING SCAN LINES GENERATED BY THE TIROS SCANNING RADIOMETER

by

James E. Arnold

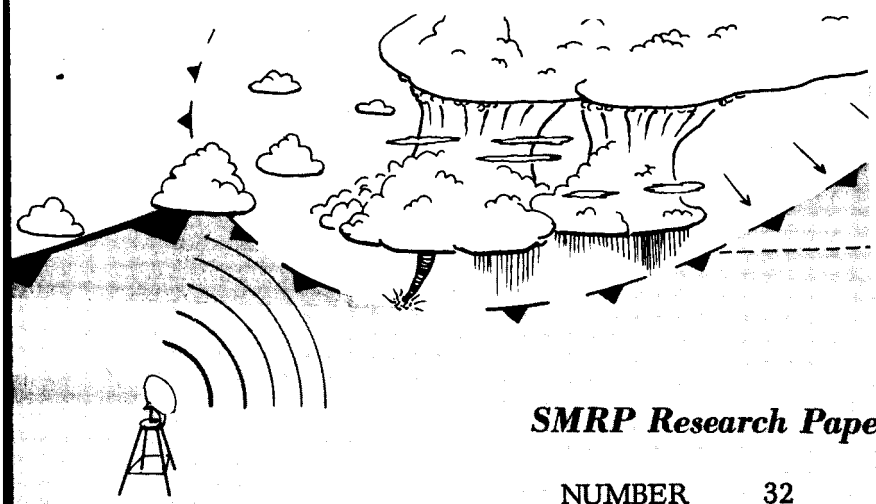

SMRP Research Paper

NUMBER 32

May 1965

MESOMETEOROLOGY PROJECT ---- RESEARCH PAPERS

1.* Report on the Chicago Tornado of March 4, 1961 - Rodger A. Brown and Tetsuya Fujita

2.* Index to the NSSP Surface Network - Tetsuya Fujita

3.* Outline of a Technique for Precise Rectification of Satellite Cloud Photographs - Tetsuya Fujita

4.* Horizontal Structure of Mountain Winds - Henry A. Brown

5.* An Investigation of Developmental Processes of the Wake Depression Through Excess Pressure Analysis of Nocturnal Showers - Joseph L. Goldman

6.* Precipitation in the 1960 Flagstaff Mesometeorological Network - Kenneth A. Styber

7.** On a Method of Single- and Dual-Image Photogrammetry of Panoramic Aerial Photographs - Tetsuya Fujita

8. A Review of Researches on Analytical Mesometeorology - Tetsuya Fujita

9. Meteorological Interpretations of Convective Nephsystems Appearing in TIROS Cloud Photographs - Tetsuya Fujita, Toshimitsu Ushijima, William A. Hass, and George T. Dellert, Jr.

10. Study of the Development of Prefrontal Squall-Systems Using NSSP Network Data - Joseph L. Goldman

11. Analysis of Selected Aircraft Data from NSSP Operation, 1962 - Tetsuya Fujita

12. Study of a Long Condensation Trail Photographed by TIROS I - Toshimitsu Ushijima

13. A Technique for Precise Analysis of Satellite Data; Volume I - Photogrammetry (Published as MSL Report No. 14) - Tetsuya Fujita

14. Investigation of a Summer Jet Stream Using TIROS and Aerological Data - Kozo Ninomiya

15. Outline of a Theory and Examples for Precise Analysis of Satellite Radiation Data - Tetsuya Fujita

* Out of print
** To be published

(Continued on back cover)

SATELLITE AND MESOMETEOROLOGY RESEARCH PROJECT
Department of the Geophysical Sciences
The University of Chicago

A SIMPLIFIED GRID TECHNIQUE FOR DETERMINING SCAN LINES GENERATED BY THE TIROS SCANNING RADIOMETER

by

James E. Arnold

SMRP Research Paper #32
May 1965

The research reported in this paper has been partially supported by the Meteorological Satellite Laboratory, U. S. Weather Bureau under grant CWB WBG-6 and by the National Aeronautics and Space Administration under grant NASA NsG 333.

A SIMPLIFIED GRID TECHNIQUE FOR DETERMINING SCAN LINES GENERATED BY THE TIROS SCANNING RADIOMETER

James E. Arnold

Department of the Geophysical Sciences
The University of Chicago
Chicago, Illinois

ABSTRACT

A grid method for the construction of scan lines generated by the TIROS scanning radiometer is presented. Making use of a series of scan line grids constructed for tilt intervals of one degree and a height range from 700 to 1000 km the user can quickly generate scan lines on an OEC projection for the geographic area in which the analysis of the radiation data is to be performed. A brief outline of the grid geometry and construction is given along with an explanation of how the grids should be used.

1. Introduction

Techniques for reducing data acquired by the scanning radiometer of the TIROS satellite have been developed by NASA, the Weather Bureau, and the University of Chicago which enable the researcher to examine meteorological systems on a global scale while maintaining the capability of resolving mesoscale meteorological systems. The fineness of the resolution, of course, depends upon the method of data reduction used and must be determined by the researcher for his particular problem. The three major ways radiation data are made available to the user are:

A. Computer reduction and presentation in the form of Grid Print Maps.

B. Final Meteorological Radiation Tape Listings (FMRT) consisting of computer reduced and located data for each satellite spin from the Master Telemetry Tapes.

C. Data reduced from analog traces reproduced from the Master Telemetry Tapes and located by computed scan lines.

The research reported in this paper has been partially supported by the Meteorological Satellite Laboratory, U. S. Weather Bureau under grant CWB WBG-6 and by the National Aeronautics and Space Administration under grant NASA NsG 333.

In practice all three methods require at least a general idea of the area scanned by the radiometer in the region of study; the more accurately this area is known, the more efficiently the data can be requested and used. It should also be remembered that because the satellite passes over an area it does not necessarily follow that the radiometer will have scanned a region the researcher might be interested in, the scanned area being a function of the satellite tilt, height, and inclination of the radiometer to the satellite spin axis. For this reason it is recommended that scan lines be constructed before requesting data covering the overpass time to determine scan boundaries and, as far as usefullness of data is concerned, the satellite zenith angles at the time of scanning.

For extensive analysis of the data once it has been located geographically it is necessary to determine such parameters as satellite zenith angle, scan spot sizes, scattering angle, and the actual viewing angle. Determination of these parameters can be accomplished quickly by graphical techniques discussed by Fujita (1963) once the scan lines through the area have been determined.

Methods of computing individual scan lines have been discussed by Fujita (1963) and Bonner (1964); the former involving a graphical solution utilizing the OEC projection, height grids, tilt grids, and a radiometer circle of an angle β , the inclination of the radiometer axis to the satellite spin axis. The latter is a computer solution of the scan geometry giving the latitude and longitude for each 10^{o} of scan angle for the scan line at a given time. Both methods are used to construct scan lines at one-minute intervals corresponding to each satellite subpoint throughout the interval of analysis. The accuracy obtained by both these methods is such that they may be considered precise in the location of data points and should be used by those requiring exact locations of radiation data.

To provide a third degree of freedom in the construction of scan lines, whether it be for time involved or the availability of computer facilities, a set of scan line grids has been developed which is of sufficient accuracy to be used for the location of scan points while enabling the scan lines to be constructed by hand in a reasonably short period of time. The scan line grids are designed to be used with the OEC chart of the scale 1^{o} of geocentric angle equal 5 mm. The grids consist of a family of scan lines constructed at an interval 1^{o} of satellite nadir angle for a height range from 700 to 1000 km for a radiometer with a $\beta = 45^{o}$.

In practice it has been found that the scan line grids are of sufficient accuracy to replace the earlier, more basic graphical method developed by Fujita except where

extremely accurate location is desired and requires considerably less time to use. It has also been found that the scan line grids generally are more convenient to use than the computer printout of scan line location when only a small number of scan lines are required.

2. Scan Line Geometry

To enable the user to better understand the scan line grids a brief review of the principles of scan geometry is in order. Those requiring a more-detailed discussion of the scanning principles should refer to Fujita (1963, 1964c).

The TIROS vehicle which carried the five-channel radiometer was a spin-stabilized craft with the radiometer axis inclined to the satellite spin axis at an angle of 45°. Each sensor consists of a floor and a wall component and when one component scans the earth the other scans space providing a reference. As the satellite travels in its orbit about the earth the angle the spin axis makes with the local vertical changes through 180° resulting in the floor component of the sensor scanning the earth for half the orbit and the wall component of the sensor scanning the earth for the remaining half as shown by Fig. 2c. When discussing the scan geometry however, it is useful to consider only the floor sensor.

To consider the scanning procedure of the TIROS radiometer it is convenient to refer to methods established for photogrammetry; that is, the transfer of the conical scan onto an image plane which is perpendicular to the satellite scan axis and then to a projection of the earth by means of a height grid. By this method the cone of rotation of the radiometer (Fig. 1) is intersected by a plane perpendicular to the radiometer's axis of rotation at a distance of $f=94.7$ mm. The circle of intersection is termed the image scan line. If now we mark azimuth lines radiating from the image subpoint at constant intervals from the image principal line and compute the intersection of cones of nadir angle from the satellite subpoint we have changed the simple image plane into a tilt or nadir angle grid for the angle of the inclination of the satellite scan axis upon which the image scan line is superimposed. By transferring the image scan line from the tilt grid to the height grid overlaying the map projection we arrive at the terrestrial scan line. Although the image scan line is circular, the terrestrial scan line may change its shape considerably. For small tilts the terrestrial scan line will be circular or near circular; however, as the satellite nadir angle increases the terrestrial scan line will become quasi-elliptical in shape on the earth and finally,

as the satellite nadir angle increases to approximately 20^{o}, a portion of the scan occurs in space and a quasi-parabolic scan line is generated on the earth. The length of the scan line on the earth is dependent on the satellite height and the satellite nadir angle and becomes larger as the satellite height increases.

The point in Fig. 1 at which the terrestrial scan line intersects the earth's horizon as the sensor rotates from aponadir to the earth's horizon is called the terrestrial first horizon while the point at which the scan line leaves the earth's surface is designated as the terrestrial second horizon. The scan lines as they appear on the image plane and on the surface of the earth are symmetric about the primary line described by the intersection of the curved surface of the earth and the plane including the satellite subpoint, primary point, and the center of the earth.

For a particular sensor the family of scan lines generated by the radiometer on the surface of the earth as the satellite travels in its orbit can be classified into three modes: Closed, Open and Alternating Open Mode. The Closed Mode phase of the scanning is encountered when the satellite nadir angle is less than approximately 20^{o}, or more specifically, when the satellite nadir angle is less than $90 - \beta - \delta_{H}$ where β is the inclination of the radiometer axis to the spin axis and δ_{H} is the horizon dip angle. In the Closed Mode, scan lines are circular or quasi-elliptical in nature with the entire spin on the earth as illustrated in Fig. 2a. It should be noted that the closed scan line on the earth permits a two-directional view of the same geographic point with only a small difference in time. As the scan nadir angle increases above 20^{o} the scanning mode is termed Open Mode and a parabolic scan line is produced on the earth's surface. When the satellite nadir angles range from about 70^{o} to 109^{o} both sensors generate scan lines on the earth as in Fig. 2b creating the Alternating Open Mode. During the Alternating Open Mode the individual scan lines that have been generated on the earth by the sensor scanning the earth becomes smaller until a last scan point is reached while simultaneously the first scan point and the succeeding scan lines are generated on the earth by the other component of the sensor. During one orbital period each of the two sensors pass through the sequence of Alternating Open Mode, Single Open Mode, Closed Mode, and back to Alternating Open Mode as illustrated in Fig. 2c.

A further breakdown of the various scan configurations may be made by considering only that portion of the scan originating at the inner or outer scan boundary and terminating at a horizon or other scan boundary. This, more specifically, reduces to separating areas on the earth that have been scanned more than once due to the changing satellite nadir angle into initial and secondary scans as illustrated in Fig. 3d.

3. Scan Line Grid Construction

The mathematical solution of the scan geometry created by the radiometer's cone of rotation as it intersects the earth has been described by Fujita (1964a) utilizing a unit sphere centered at the satellite. Knowing η. and Ψ. , the nadir angle and scan angle of the scan point (Fig. 1) its latitude-longitude position on the earth can be computed by solving a set of spherical triangles by computer methods.

For the transfer of the image scan line to the terrestrial sphere by graphical methods a tilt grid and height grid of either an Oblique Equidistant Cylindrical projection (OEC) or a Zenith Equidistant projection (ZE) may be used. As has been mentioned previously, the use of an OEC height grid permits great accuracy in the location of the scan points as does the computer location of the points; however, the use of the OEC height grid necessitates a minimum rotation of the grid to maintain its designed accuracy, which when constructing a single scan line grid method cannot be practically incorporated.

To solve the problem of grid rotation the ZE height grid was used. The radials of the ZE height grid are straight lines approximating the true meridians on the earth as opposed to being actual representations as is the case of the OEC height grid. This approximation results in a small tangential error which reaches a maximum at 54^{o} of rotation and has a value of 78 km at the horizon for a satellite height of 700 km. This seemingly large error at the horizon angle of 64.7^{o} from the subpoint falls off rapidly as the distance increases from the horizon such that at a nadir angle of 50^{o} from the subpoint it reaches 2.5 km and becomes nearly 0 for subpoint nadir angles less than 40^{o}. The nature of this error is more graphically illustrated in Fig. 3 where it can be seen that it is only at the horizon, in the vicinity of the maximum error, that the tangential error approaches a magnitude that should be considered. Even here the magnitude of the error is not so important as might first be thought since the data at the horizon points are generally badly distorted and not usable. There is also a small radial error, but this error is much smaller than the tangential error and need not be considered. A more detailed discussion of the errors involved in using the various grids was undertaken by Fujita (1964b) and interested readers should refer to that work.

Using the tables of scan nadir and horizontal angles for a β of 45^{o} at each 10^{o} of satellite spin angle determined by Bonner (1964) and the ZE height grid, Scan Line Grids were constructed through a nadir angle range from 0 to 109^{o} in 1^{o} intervals for a height range from 700 to 1000 km for 20 km intervals. Each 1^{o} grid interval

consists of a family of scan lines with every 10^{o} of azimuth marked from the perinadir. To prevent overlapping scan lines at a single nadir angle the grid position of the subpoint corresponding to a scan line of that nadir angle at a given height was shifted along the grid primary line for the nadir angle interval from 14^{o} to 100^{o}. This resulted in a height scale to be placed on the subpoint along the grid primary line which corresponds to a height scale on the grid scan lines for the interval under discussion while the remaining grids have a single grid subpoint. Examples of scan line families for four different satellite nadir angles are shown in Fig. 4 where the following features should be noted. As previously pointed out grids constructed for angles less than 15^{o} and greater than 100^{o} have a single satellite subpoint on the grid primary line. Grids constructed within the interval between 15^{o} and 100^{o} have a satellite subpoint position on the grid primary line corresponding to the actual satellite height, at the time the scan line is generated.

Each scan line in the family of scan lines at a given tilt corresponds to a different satellite height. As the satellite height increases the distance from the subpoint to the corresponding scan line also increases such that on the scan line grid the innermost line, considering the zero satellite height as a focus point, is the scan line generated for a satellite height of 700 km while the outermost line is the scan line generated for a satellite height of 1000 km.

Since it is necessary to know the sensor's angle of rotation from the aponadir (spin angle) when it crosses over the apparent horizon for transferring the latitude and longitude grid from the OEC projection to various printout forms (see Fig. 4), graphs I and II were computed. These graphs give the spin angle at which the sensor crosses the first horizon measured from the aponadir as a function of satellite height and the nadir angle of the spin axis. It should be recalled that the scan line is symmetric about the primary line so the crossing angle of the second horizon may be obtained by simply subtracting from 360^{o} the spin angle of the first horizon.

4. Use of the Scan Line Grids

Construction of scan lines on the OEC chart using the scan line grids requires:

1. Orbital subpoint data and satellite height for the time period that scan lines are to be constructed.
2. Satellite spin axis points on the terrestrial sphere.
3. Primary lines and the satellite nadir angles for the time period scan lines are to be constructed.

In the construction of the primary lines on the OEC chart it will be noted that primary lines, except where the minimum nadir angle is nearly 0^{o} or when the area in which the primary lines are drawn is very close to the minimum nadir angle are slightly curved. Since the grid primary line is straight (a ZE projection characteristic), it has been found convenient to limit the length of the primary line on the OEC projection to about 15^{o} of geocentric angle. This will facilitate easier allignment of the grid primary lines with the primary lines constructed on the OEC projection. Prior to actual construction of the scan lines on the OEC chart the user should draw on the OEC chart the primary lines covering the interval that scan lines are to be constructed and should determine and label the satellite height and nadir angle at each scan time. As mentioned before and as is shown in Fig. 5, the height of the satellite should be taken into account in placing most of the scan line grids and for the reproduction of the scan line.

To construct the scan lines the scan line grid corresponding to the satellite tilt at that time is placed under the OEC chart. Placing the correct satellite height on the grid primary line under the satellite subpoint, the grid should then be rotated until the grid primary line and the projection primary line coincide. Then the scan line in the family of scan lines corresponding to the satellite height is located and each 10^{o} of spin angle marked and the scan line drawn as shown in Fig. 6. This procedure is repeated for each scan line to be drawn.

Because the satellite nadir angle seldom if ever changes at 1^{o} intervals it becomes necessary to combine two scan line grids of successive tilt to obtain accurate placement of the scan line on the OEC chart. This will be found desirable in most cases when the satellite nadir angle differs more than about 0.2^{o} from a grid tilt value. The type of error introduced by using only the 1^{o} interval varies with the satellite nadir angle and the position in the scan. For a better illustration of this, Fig. 7 should be referred to. It can be seen that for small nadir angles the largest error occurs near the perinadir and aponadir. The error at the aponadir reaches a maximum in the vicinity of the horizon just as the scan line is opening into space. For example, in the case of a nadir angle change from 18 to 19^{o} this error is on the order of 5^{o} of geocentric angle (about 555 km). As the satellite nadir angle approaches 45^{o} the error resulting from a change of nadir angle over a small interval reaches a minimum, after which it begins to increase.

It should be apparent that accurate location of data points along the scan line in many cases will require interpolation between two scan line grids. The method used to interpolate the specific scan line is up to the individual user; however, it

has been found convenient to construct a new grid for the scan line by drawing the two whole degree scan lines on a single sheet of paper and interpolating the desired scan line and then transferring this line to the OEC chart.

Completion of a set of scan lines on the OEC chart by the use of the scan line grids should permit the user to locate radiation data accurately enough for all but the most exacting work with a minimum amount of effort and time spent constructing scan lines. It also permits a rapid check of available coverage at a given portion of the orbit and separation of scan lines into initial and secondary scans. The determination of scan aspects such as satellite zenith angle and scan spot scan also follow quickly once the scan lines have been determined. For practical purposes it is impossible to include copies of the 109 scan line grids in this report, however, those wishing complete sets should address their inquiries to the Satellite and Mesometeorology Research Project, University of Chicago.

REFERENCES

Bonner, William, 1964: Tables of scan nadir and horizontal angles. SMRP Research Paper 31, Univ. of Chicago.

Fujita, T., 1963: Outline of a theory of examples for precise analysis of satellite radiation data. SMRP Research Paper 15, Univ. of Chicago.

_____, 1964a: A technique for precise analysis of satellite data, Vol. II - Radiation analysis, Section 6. Fixed-position scanning. SMRP Research Paper 29, Univ. of Chicago.

_____, 1964b: Evaluation of errors in the graphical rectification of satellite photographs. SMRP Research Paper 30, Univ. of Chicago.

_____, 1964c: The scanning printer and its application to detailed analysis of satellite radiation data. SMRP Research Paper 34, Univ. of Chicago.

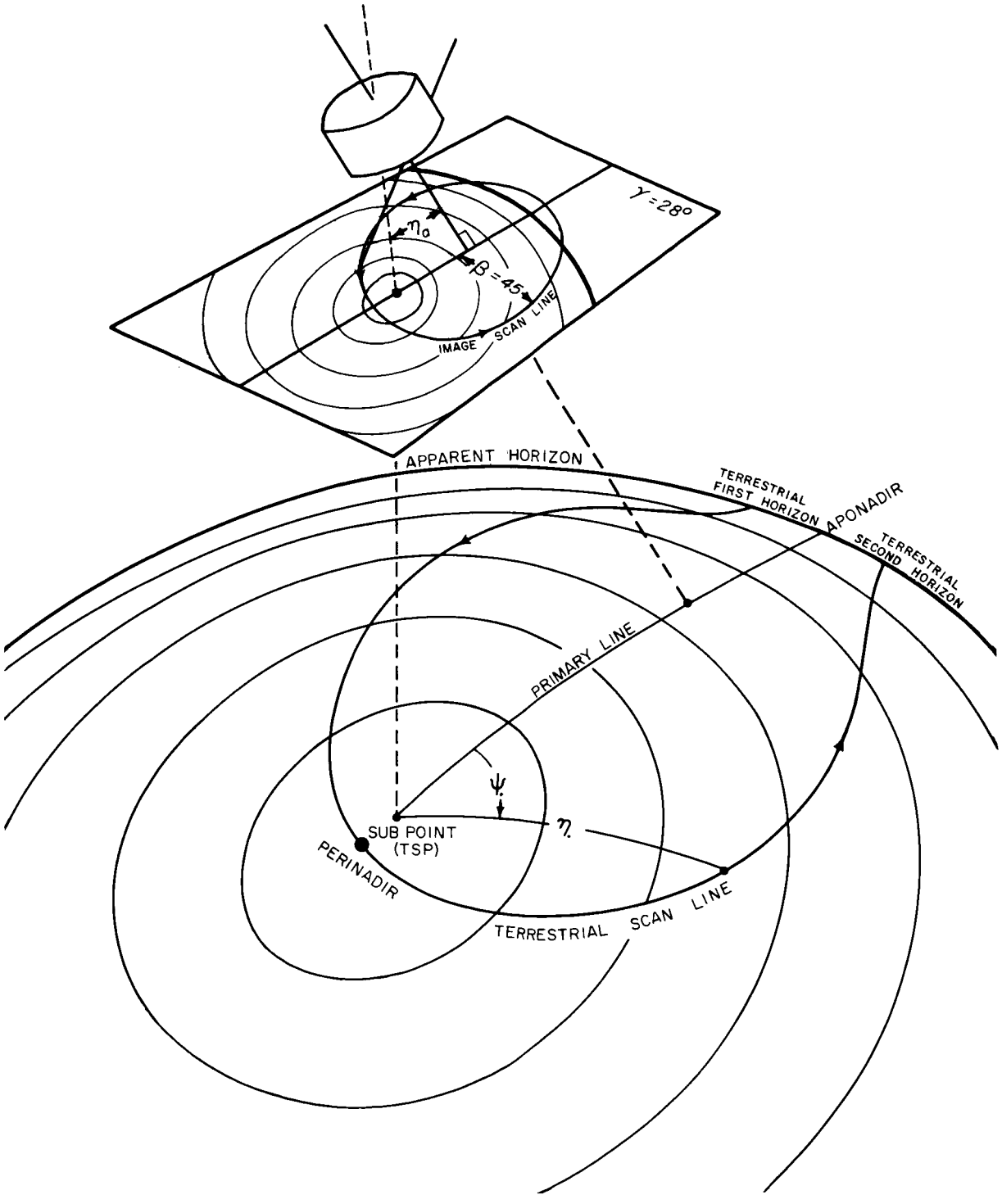

Fig. 1. Scan configuration of the Terrestrial and Image Scan Line.

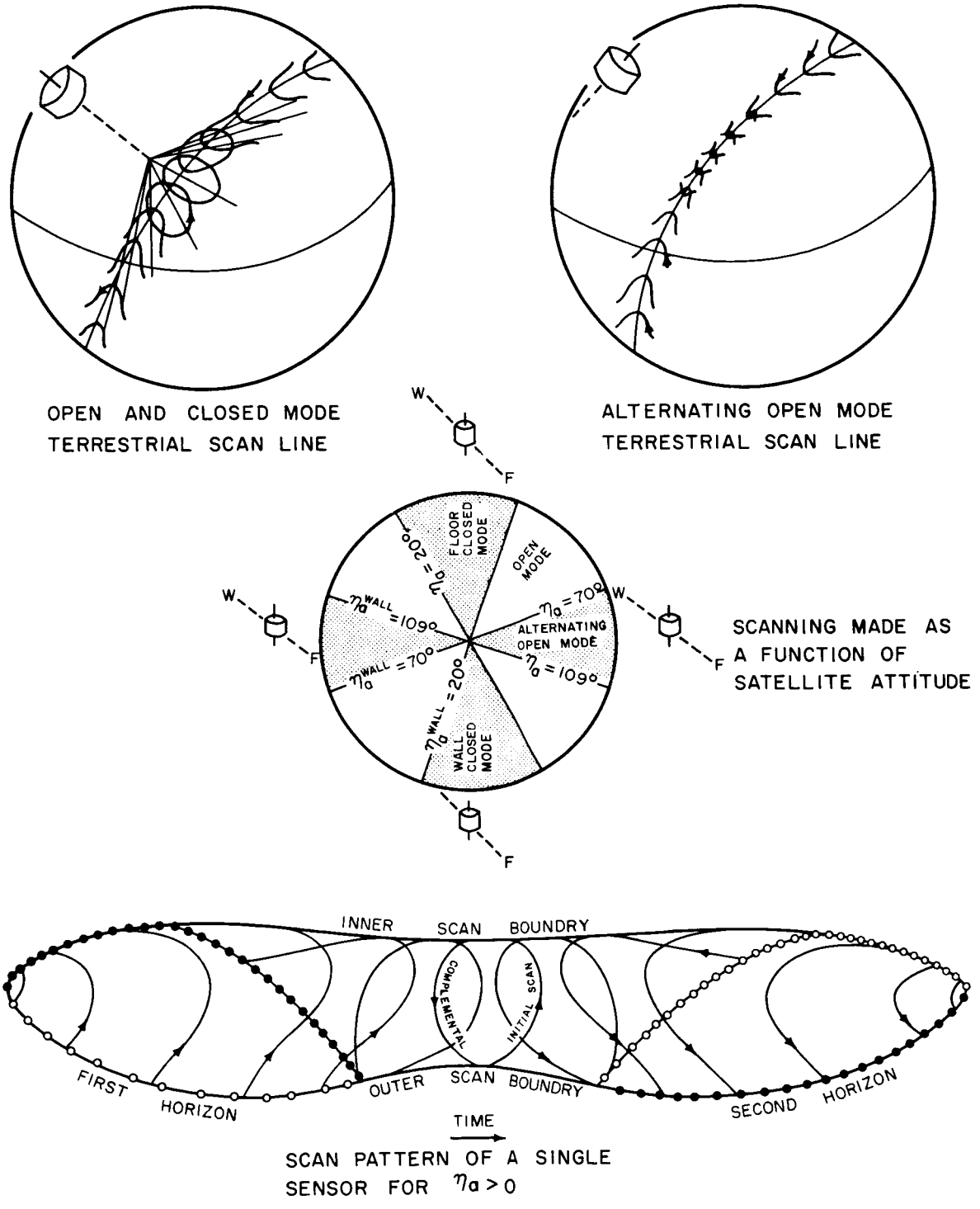

Fig. 2. Pictorial display of the TIROS scanning modes and scan configuration.

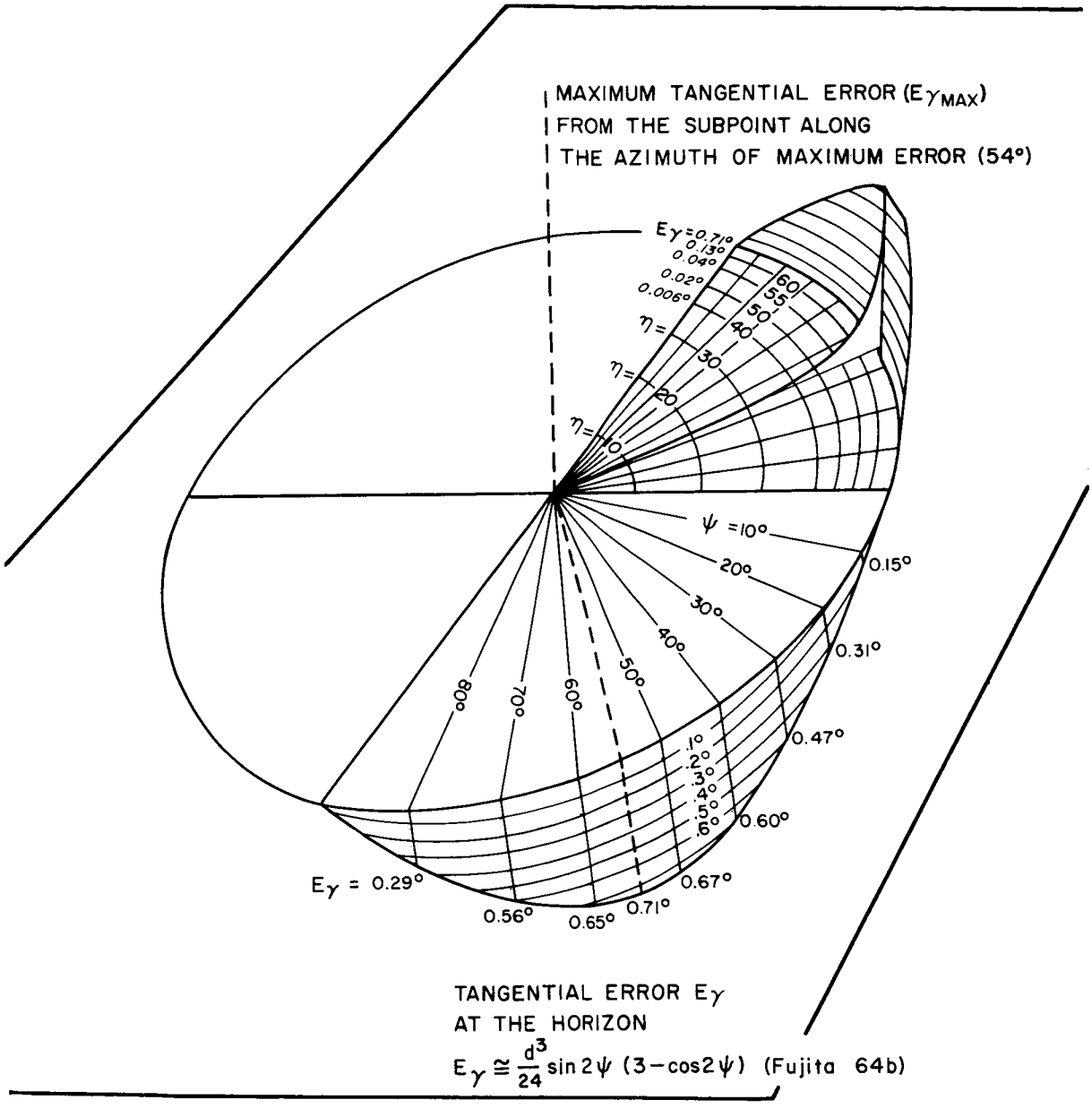

Fig. 3. Tangential error in the scan line grid construction created by the use of the Zenith Equidistant Height grid.

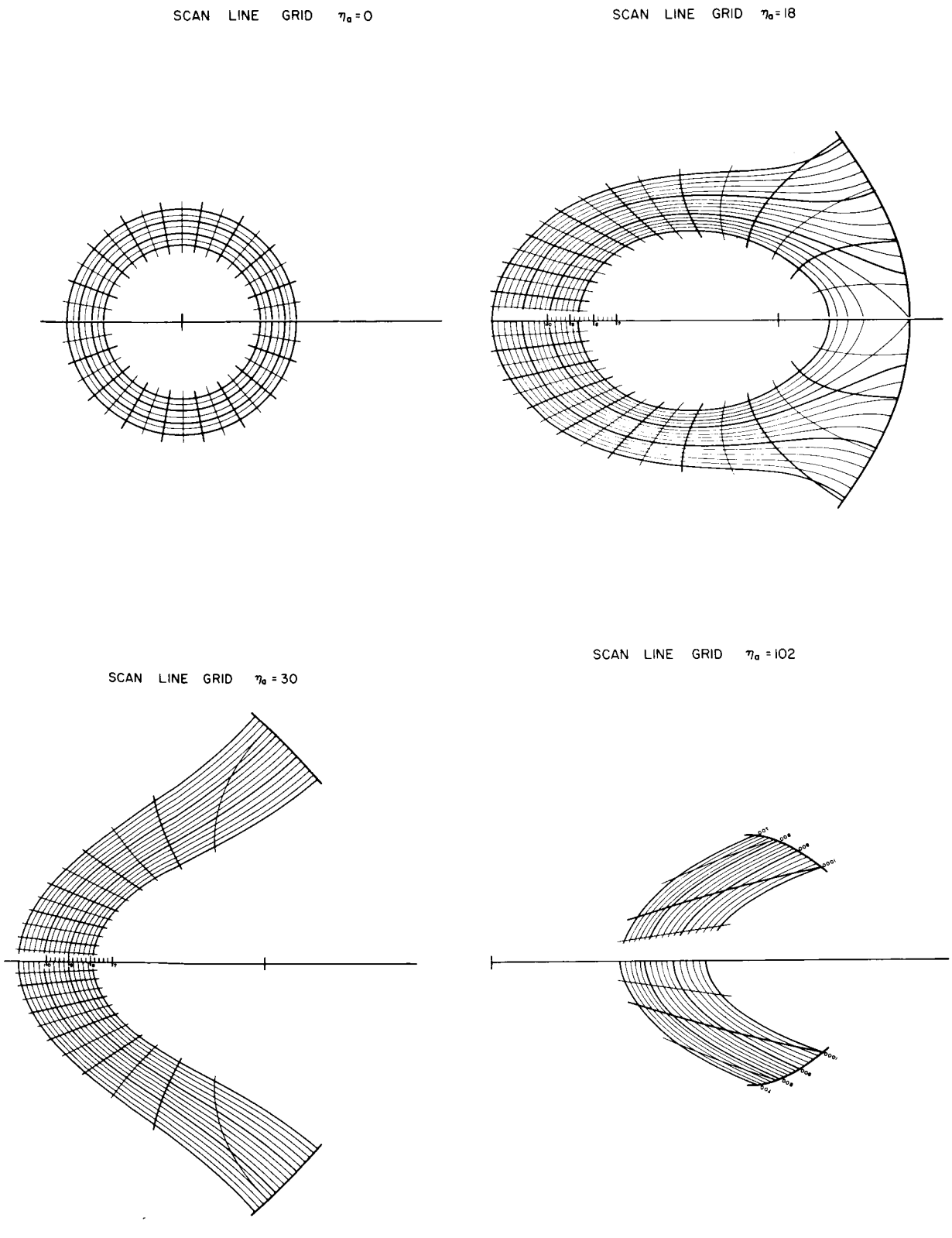

Fig. 4. Representative examples of scan line grids illustrating the change in scan line shape with increasing scan axis nadir angle.

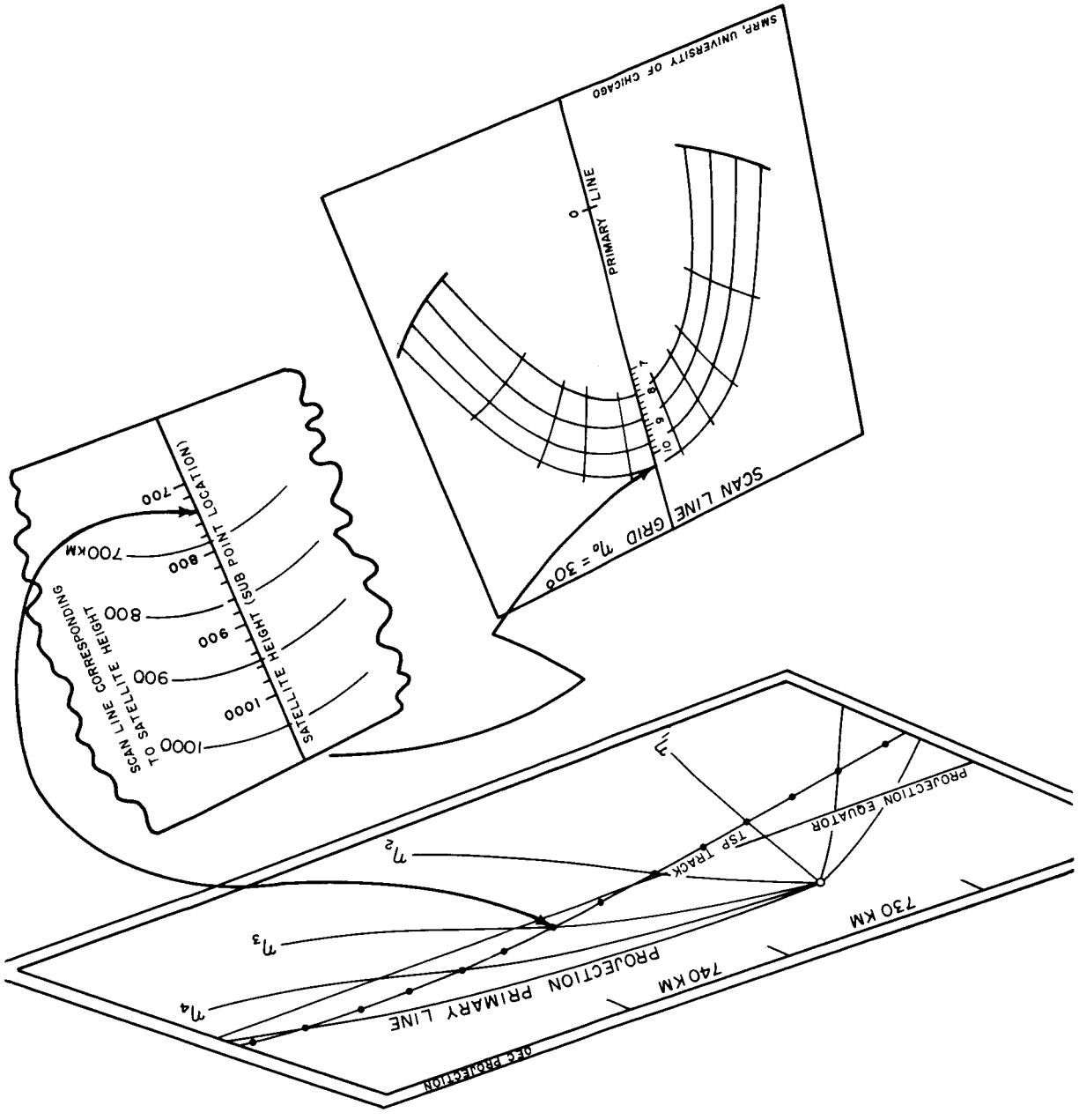

Fig. 5. Construction of the scan line on the OEC projection requires the determination of the projection primary line, satellite nadir angle, and proper placement and orientation of the scan line grid.

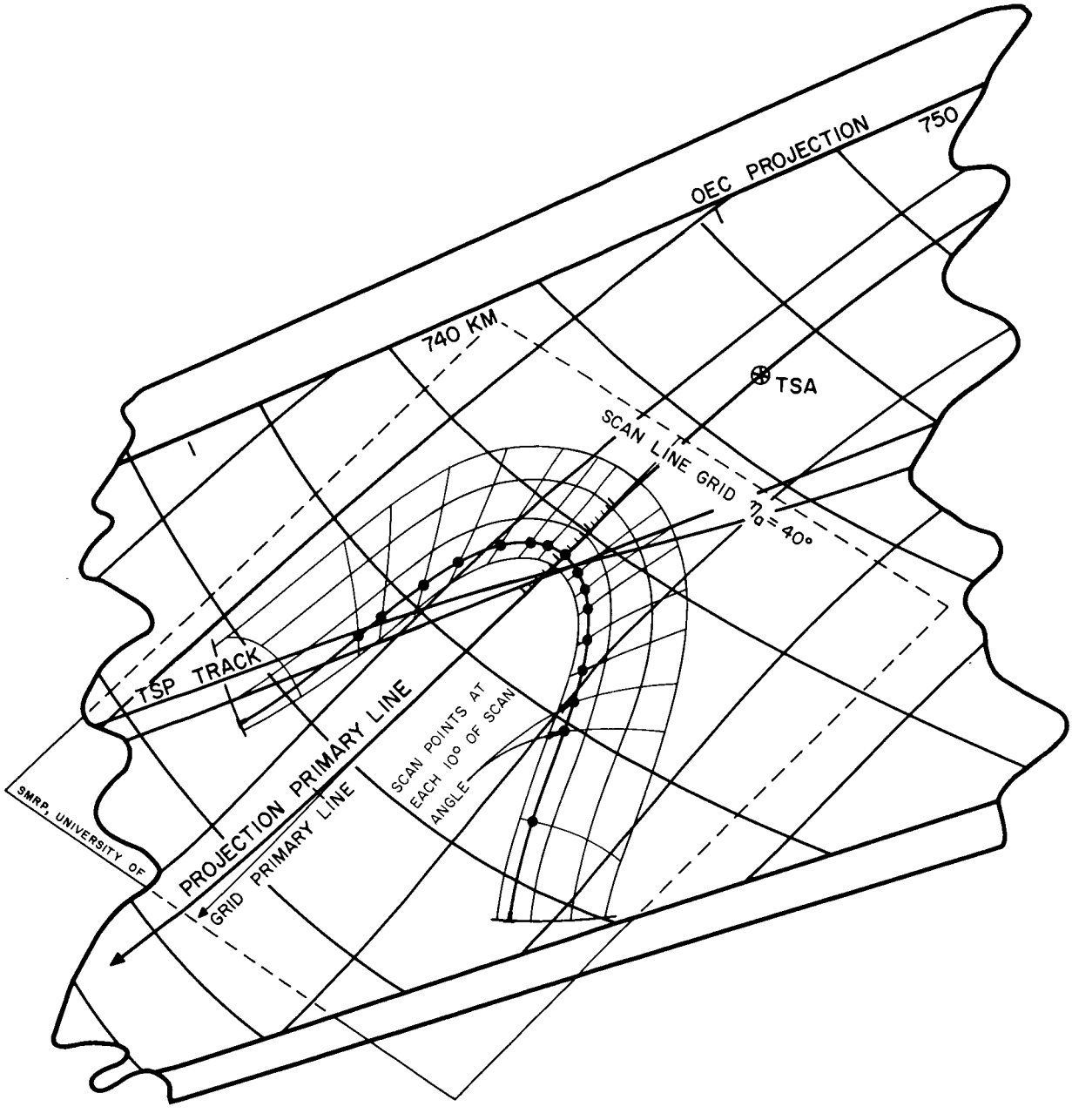

Fig. 6. Construction of the Terrestrial Scan Line on the OEC projection.

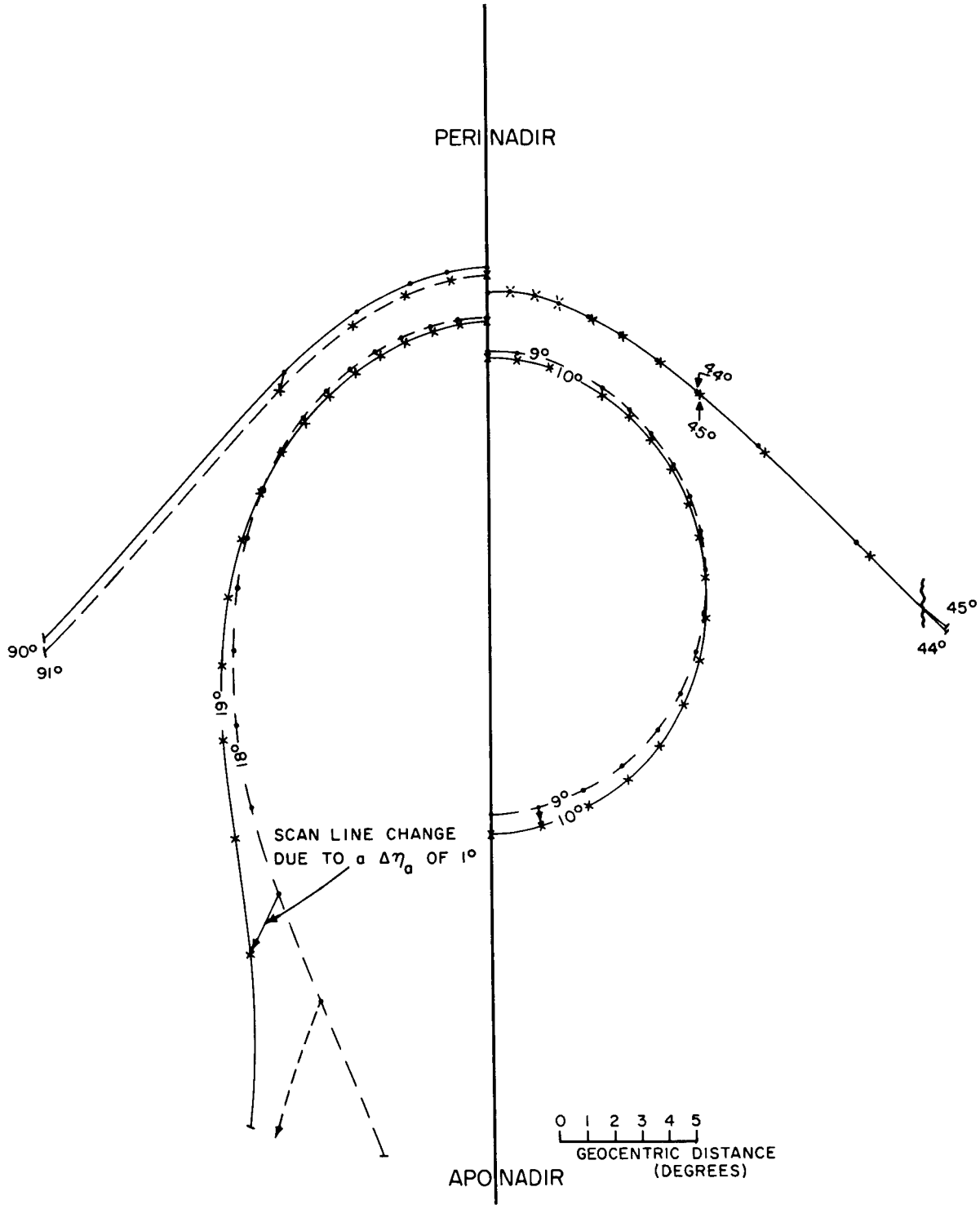

Fig. 7. Vector difference for four selected pairs of scan lines illustrating the effect of a 1^{o} change of scan axis nadir angle in grid construction.

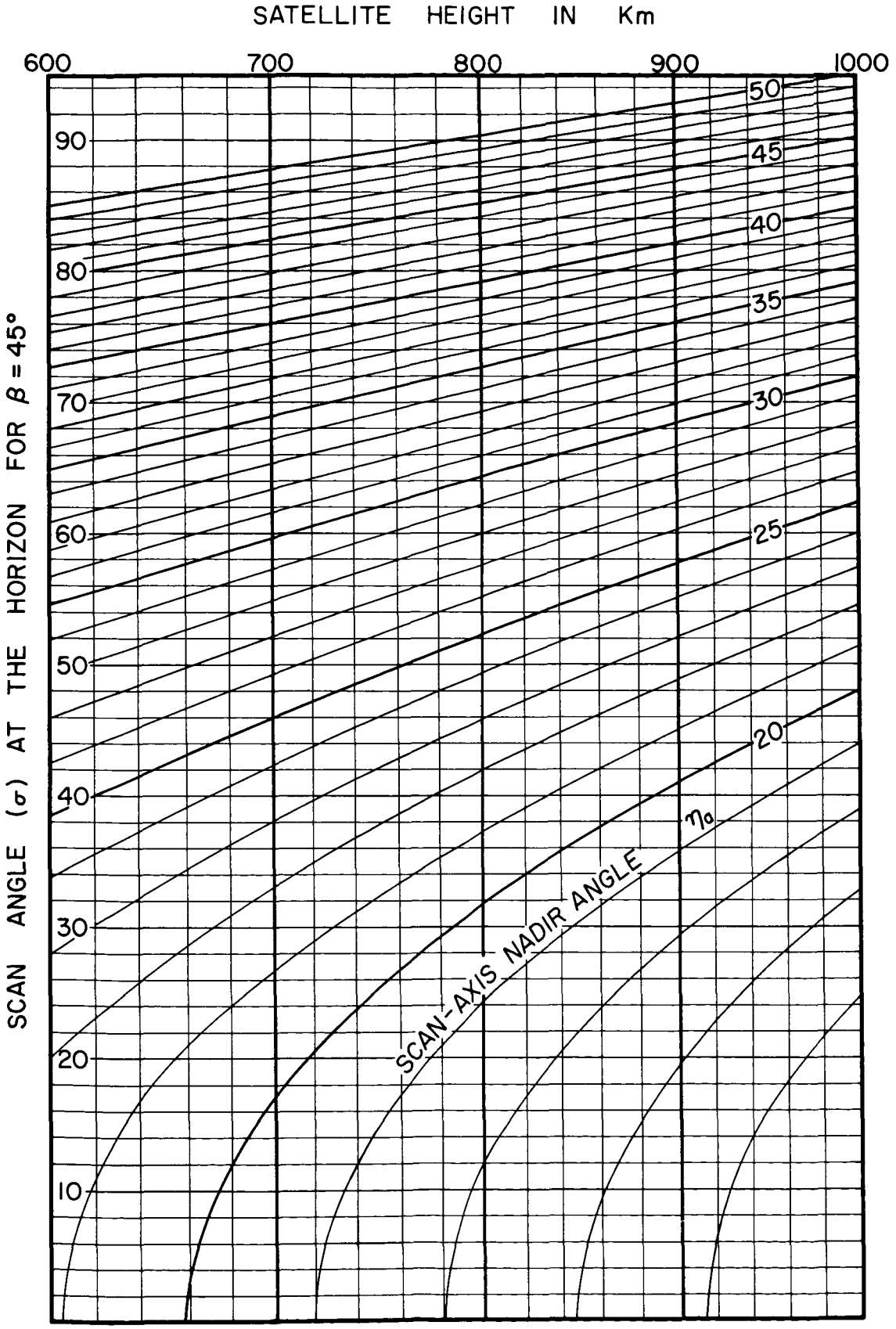

Fig. 8. A nomogram (graph) of scan angle at the horizon as a function of scan-axis nadir angle and satellite height for scan nadir angles from 0° to 50°.

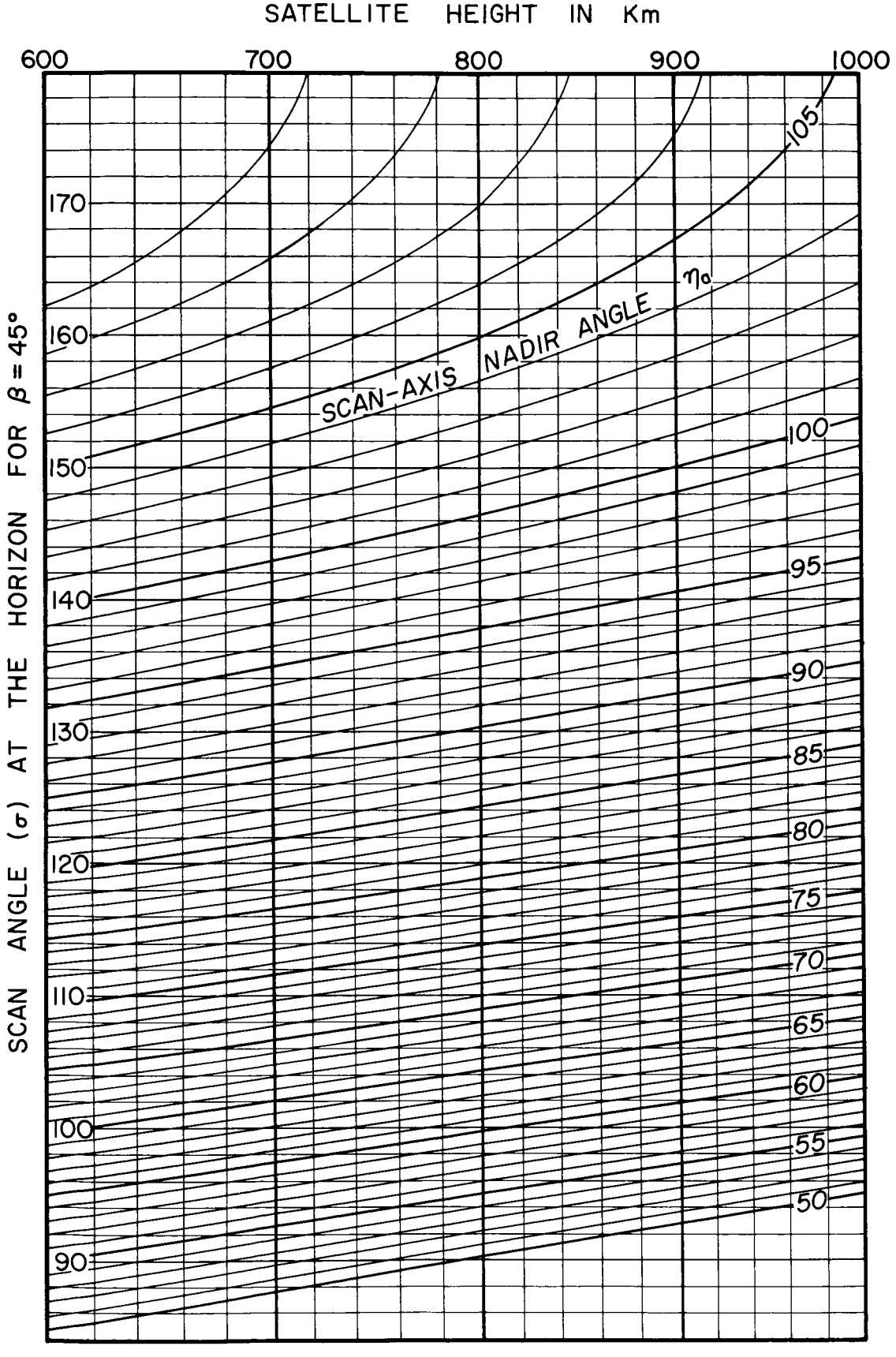

Fig. 9. A nomogram (graph) of scan angle at the horizon as a function of scan-axis nadir angle and satellite height for scan nadir angles from 50° to 109°.

MESOMETEOROLOGY PROJECT - - - - - RESEARCH PAPERS

(Continued from front cover)

16. Preliminary Result of Analysis of the Cumulonimbus Cloud of April 21, 1961 -Tetsuya Fujita and James Arnold

17. A Technique for Precise Analysis of Satellite Photographs - Tetsuya Fujita

18. Evaluation of Limb Darkening from TIROS III Radiation Data - S.H.H. Larsen, Tetsuya Fujita, and W. L. Fletcher

19. Synoptic Interpretation of TIROS III Measurements of Infrared Radiation -Finn Pedersen and Tetsuya Fujita

20. TIROS III Measurements of Terrestrial Radiation and Reflected and Scattered Solar Radiation - S.H.H. Larsen, Tetsuya Fujita, and W.L. Fletcher

21. On the Low-level Structure of a Squall Line - Henry A. Brown

22. Thunderstorms and the Low-level Jet - William D. Bonner

23. The Mesoanalysis of an Organized Convective System - Henry A. Brown

24. Preliminary Radar and Photogrammetric Study of the Illinois Tornadoes of April 17 and 22, 1963 - Joseph L. Goldman and Tetsuya Fujita

25. Use of TIROS Pictures for Studies of the Internal Structure of Tropical Storms -Tetsuya Fujita with Rectified Pictures from TIROS I Orbit 125, R/O 128 -Toshimitsu Ushijima

26. An Experiment in the Determination of Geostrophic and Isallobaric Winds from NSSP Pressure Data - William Bonner

27. Proposed Mechanism of Hook Echo Formation - Tetsuya Fujita with a Preliminary Mesosynoptic Analysis of Tornado Cyclone Case of May 26, 1963 -Tetsuya Fujita and Robbi Stuhmer

28. The Decaying Stage of Hurricane Anna of July 1961 as Portrayed by TIROS Cloud Photographs and Infrared Radiation from the Top of the Storm -Tetsuya Fujita and James Arnold

29. A Technique for Precise Analysis of Satellite Data, Volume II - Radiation Analysis, Section 6. Fixed-Position Scanning - Tetsuya Fujita

30. Evaluation of Errors in the Graphical Rectification of Satellite Photographs -Tetsuya Fujita

(Continued on outside)

MESOMETEOROLOGY PROJECT - - - - - RESEARCH PAPERS

(Continued from inside)

31. Tables of Scan Nadir and Horizontal Angles - William D. Bonner